



## Contribution of intragenic deletions to mutation spectrum in Chinese patients with Wilson's disease and possible mechanism underlying *ATP7B* gross deletions

Yu-Chao Chen<sup>a,b,1</sup>, Hao Yu<sup>a,1</sup>, Rou-Min Wang<sup>a,1</sup>, Juan-Juan Xie<sup>a</sup>, Wang Ni<sup>a</sup>, Yue Zhang<sup>c</sup>, Yi Dong<sup>a,\*\*</sup>, Zhi-Ying Wu<sup>a,\*</sup>

<sup>a</sup> Department of Neurology and Research Center of Neurology in Second Affiliated Hospital, and Key Laboratory of Medical Neurobiology of Zhejiang Province, Zhejiang University School of Medicine, Hangzhou, China

<sup>b</sup> Department of Neurology and Institute of Neurology, First Affiliated Hospital, Fujian Medical University, Fuzhou, China

<sup>c</sup> Department of Neurology and Institute of Neurology, Huashan Hospital, Shanghai Medical College, Fudan University, Shanghai, China

### ARTICLE INFO

#### Keywords:

Wilson's disease  
*ATP7B*  
Intragenic deletion  
Breakpoint

### ABSTRACT

**Introduction:** Wilson's disease (WD) is an autosomal recessive disorder of copper metabolism due to *ATP7B* pathogenic mutations. Disease manifestations can be prevented if early diagnosis and effective treatment are given. Direct sequencing is routinely used to confirm WD diagnosis, but cannot identify gross rearrangements. **Methods:** Sanger sequencing of *ATP7B* was performed in 142 newly recruited WD index patients. The clinical effects of identified variants were classified according to American College of Medical Genetics and Genomics (ACMG) standards and guidelines. Multiplex ligation-dependent probe amplification (MLPA) was performed in 168 WD cases with clinical WD unexplained by Sanger sequencing, selected from our total case series of 774 WD patients. After identifying gross rearrangements within *ATP7B*, the breakpoints were determined by long-range PCR and direct sequencing.

**Results:** In the 142 WD patients, we identified 71 sequence alterations in *ATP7B*, of which 15 were novel; 14 of these were classified as 'pathogenic' or 'likely pathogenic', including 2 intronic variants affecting splice sites. In 6 of 168 WD patients, MLPA identified four heterozygous gross *ATP7B* deletions. One was a whole gene deletion, and three were intragenic deletions which were mapped to breakpoint locations, revealing non-homologous end joining.

**Conclusion:** Intragenic deletions are responsible for WD and non-homologous end joining could be the pathogenesis, therefore the detection of intragenic deletions should be included in comprehensive genetic testing for WD.

### 1. Introduction

Wilson's disease (WD) is an autosomal recessive disorder of copper overload, characterized by damaged incorporation of copper into apoceruloplasmin and decreased biliary excretion of copper into bile [1]. Massive copper accumulations in various organs or tissues cause complicated clinical heterogeneity, predominantly manifesting as different kinds of hepatic, neurologic, and psychiatric diseases. Mutations in the *ATP7B* gene, which encodes a copper-transporting ATPase in the liver, are responsible for disease onset [2].

WD could be lethal if left untreated. Fortunately, it is also treatable under the condition of lifelong copper-chelating therapy and dietary copper restriction. If WD patients receive standardized medications, they could be largely presymptomatic for the rest of life. Therefore, the early and timely diagnosis is essential for affected individuals. The diagnosis of WD is based on a combination of clinical symptomology and laboratory tests. Ultimately, the confirmation depends on the identification of the disease-causing mutations [3]. According to Human Gene Mutation Database Professional (<https://portal.biobase-international.com/hgmd/pro/gene.php?gene=ATP7B>, access date: March, 2018),

\* Corresponding author.

\*\* Corresponding author. Department of Neurology and Research Center of Neurology in Second Affiliated Hospital, and Key Laboratory of Medical Neurobiology of Zhejiang Province, Zhejiang University School of Medicine, 88 Jiefang Rd, Hangzhou, 310009, China.

E-mail addresses: [dongyi720@zju.edu.cn](mailto:dongyi720@zju.edu.cn) (Y. Dong), [zhiyingwu@zju.edu.cn](mailto:zhiyingwu@zju.edu.cn) (Z.-Y. Wu).

<sup>1</sup> These three authors contributed equally to this work.

approximately more than 800 *ATP7B* variants with different clinical effects have been described. Additionally, in a fraction of clinical confirmed WD patients, only one disease allele was identified, or even none [4]. These confusions consequently pose diagnostic challenges.

There are many ongoing studies focusing on characterizing mutations within *ATP7B*. Besides the common single-base substitutions or small indels via Sanger sequencing, few data are available regarding *ATP7B* gross rearrangements. To date, only a few intragenic rearrangements were identified among different ethnic groups [5–11]. Although there was one study mentioning gross deletion in Chinese WD patients [12], detailed sequence information was not described.

In this study, we aimed at collecting more WD patients and further expanding the mutation spectrum to facilitate genetic diagnosis. Moreover, since Sanger sequencing technique is unsuitable for detecting gross arrangements, multiplex ligation-dependent probe amplification (MLPA) assay was performed to identify WD patients carrying large deletions or duplications. Additionally, we further investigated the specific *ATP7B* breakpoints and mechanism underlying the occurrence of intragenic rearrangements.

## 2. Materials and methods

### 2.1. Subjects

Between April 2015 and August 2017, we collected 142 unrelated WD patients referred to our diagnosis and treatment center at Second Affiliated Hospital of Zhejiang University School of Medicine. The clinical diagnosis was made according to the Leipzig Score [3]. Each patient was evaluated for clinical history and physical examination by two senior neurologists. Besides these newly recruited patients, we also recruited 148 patients from the previous WD cohorts, including 63 cases without definite genetic diagnosis (58 with “only one mutation” and 5 with “no mutation”), and 85 homozygotes without genetic confirmation of parents [13] (Supplemental Fig. 1). The study was approved by the ethics committee of Second Affiliated Hospital, Zhejiang University School of Medicine. The informed consents were obtained by the participants or their guardians.

### 2.2. Mutation screening

Genomic DNA was extracted from peripheral blood using a DNA isolation kit (Qiagen Inc, Valencia, CA). The entire coding regions and exon/intron boundaries within *ATP7B* were amplified using primers as previously described [13]. PCR amplification and bidirectional sequencings were performed. After failing to identify biallelic pathogenic variants, the *ATP7B* remainders, including promoter, 5'- untranslated region (UTR) and 3'UTR, were further analyzed. All detected sequences were compared to the reference (NM\_000053.3) from NCBI, and nucleotide changes were numbered. When identifying the novel sequence variant, the pathogenicity was determined based on the American College of Medical Genetics and Genomics (ACMG) Standards and Guidelines [14].

### 2.3. MLPA analysis

To detect whether large rearrangements occurred within *ATP7B* in our cohort study, we conducted MLPA analysis in all clinically confirmed patients carrying “one mutation”, “no mutation” or “suspected homozygous mutations”. The targeted fragments (5'UTR to exon 21) were amplified using a commercially available MLPA kit (Salsa P098-C2; MRC-Holland, Netherlands) according to the manufacturer's protocol, and then loaded on the ABI 3500xL Dx Genetic Analyzer. The acquired data were further analyzed via [Coffalyser.net](http://Coffalyser.net) V03 software (MRC-Holland). Repetitive screenings were performed to avoid false positive results.

### 2.4. Breakpoint mapping using long-range PCR

After detecting gross *ATP7B* deletions, we further specified the deletion breakpoint using long-range PCR and direct sequencing. Long-range PCR was performed according to the manufacturer's instructions of KOD FX Neo (TOYOBO, Japan). The corresponding primers were designed to locate the exons, upstream and downstream of the targeted region (Supplemental Table 1). Because of large-size intron 1, it's inappropriate to perform long-range PCR directly. Therefore, we selected some single-nucleotide polymorphisms (SNPs) which are exclusive in Asia population retrieved from the HapMap Genome Browser, and further genotyped SNPs (Supplemental Table 2). If certain SNPs held heterozygous state, we could confirm that the deletion region did not cover this zone, so that to narrow down the target fragment. Finally, direct sequencing was used to match and confirm the finding.

## 3. Results

### 3.1. Variants identified among 142 patients and pathogenicity classification

A total of 71 genetic variants within *ATP7B*, including 42 missenses, 5 nonsenses, 9 splicing sites, and 15 small deletions/insertions, were identified among 142 patients. Among 71 variants, 56 have been reported and classified as disease-causing mutation [13] (Supplemental Fig. 2). The remaining 15 variants were firstly reported around the world (Fig. 1A), none of which was detected in previously reported 503 normal controls [13].

Among these novel variants (Table 1), there was one nonsense variant, c.2692C > T (p.Q898X), which resulted in a truncated premature *ATP7B* protein and was classified as a ‘pathogenic variant’ according to ACMG Standards and Guidelines. Three splice site variants were detected, of which c.51+2T > G and c.4124+2T > G were predicted to induce defective protein due to exon skipping, hence were classified as ‘pathogenic variants’, while c.4124+4A > G was only classified as a ‘variant with uncertain significance’. Three small insertions, including c.171\_174dup (p.T59Gfs\*20), c.192\_193dup (p.L65Sfs\*4) and c.326dup (p.Q110Afs\*53), could be classified as ‘pathogenic variants’ due to the production of truncated *ATP7B* protein. Like missense variant, the variant of c.2212\_2213delinsCA (p.S738H) only caused the transformation from serine to histidine, therefore being classified as ‘likely pathogenic variant’. Additionally, 7 missense variants were classified as ‘pathogenic variant’ or ‘likely pathogenic variant’. Homology analysis among various species showed missense variants occurred within highly conserved regions of *ATP7B* protein (Fig. 1B). In total, 14 novel variants were considered as potential disease-causing mutations and the remaining one as variant with uncertain significance.

Consequently, among 142 WD patients, 127 (89.4%) were identified with homozygous (19 patients) or compound heterozygous (108 patients) at this stage. Of another 15 patients, 5 were identified with one causative mutation and another uncertain variant, 9 with only one causative mutation and one without any mutation. Therefore, after the direct sequencing analysis, we further screened these 15 patients using MLPA assay. Additionally, 5 out of 19 homozygotes were also included because of no parental genetic confirmation.

### 3.2. Four novel large deletions were identified in six index patients

MLPA analysis was totally performed among 168 patients including 148 previously reported patients [13]. The Results showed that 4 large deletions within *ATP7B* were identified in 6 patients, who had two different genetic results (‘homozygous pathogenic variants detected’ without parental confirmation and ‘one or none pathogenic variant detected’) (Supplemental Fig. 1, Supplemental Table 3). The intragenic deletion was not identified in the newly recruited WD patients.

Patient 1 and 2 were found to carry a heterozygote of exons 10-11

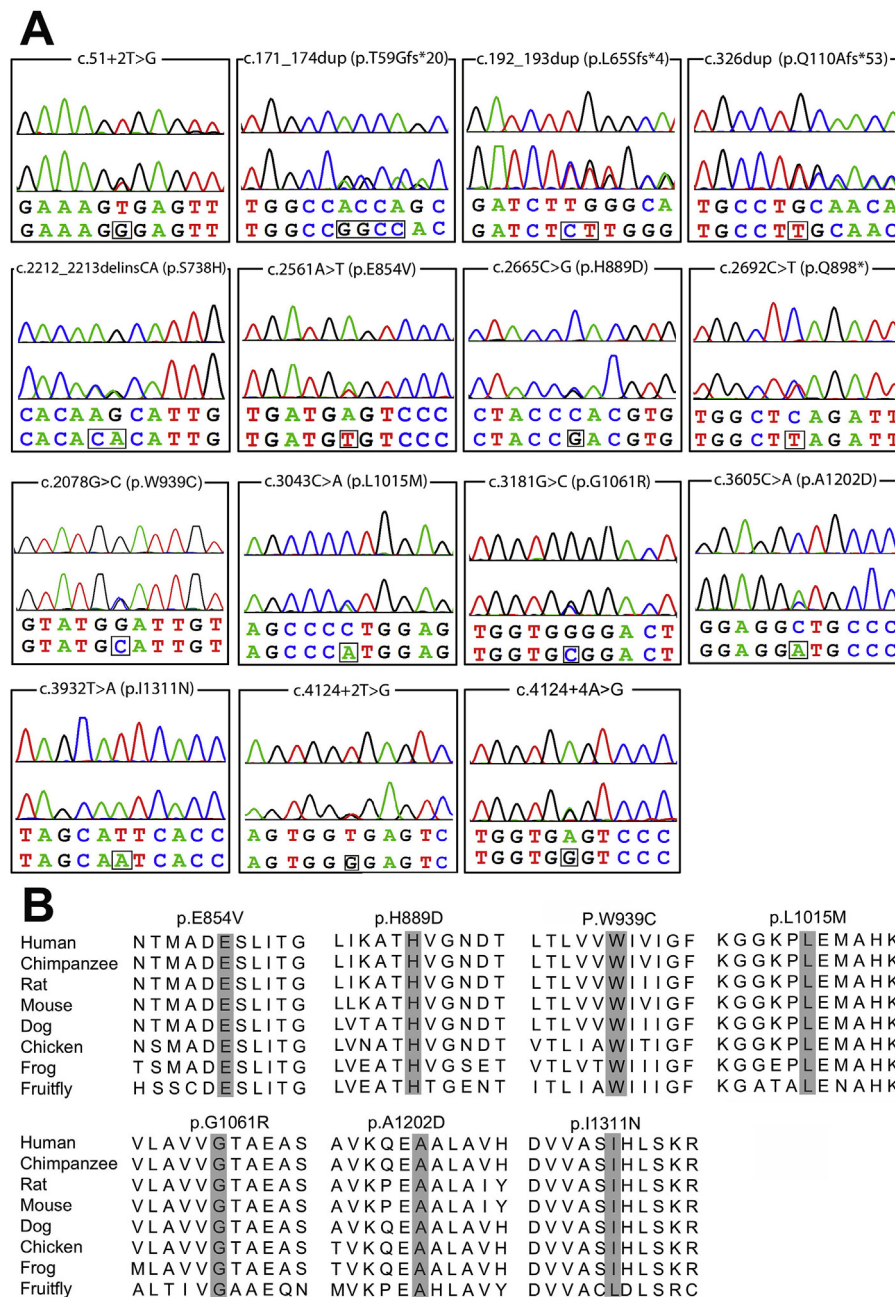


**Fig. 1. Sequencing chromatograms and conservation analysis of novel ATP7B variants.** A. Sequencing chromatograms of 15 novel ATP7B variants. The upper sequence in each frame represents the normal sequence, whereas the lower one represents the variant. B. Conservation analysis of 7 novel missense variants. The highlighted zones respectively indicate 7 variant sites among 8 diverse species.

deletion (Supplemental Fig. 3A). Similarly, two unrelated patient 3 and 4 harbored a heterozygous deletion of exon 2 (Supplemental Fig. 3B), while patient 5 carried the mutation of exons 18-21 deletion (Supplemental Fig. 3C). Unexpectedly, we found through MLPA analyses that patient 6, whom we previously considered to be homozygote for p.T935M, actually had a heterozygous whole-exon (5'UTR-exon21) deletion, combined with a heterozygous p.T935M mutation on the other allele. (Fig. 2A). However, the affected genes in the vicinity of ATP7B were undetermined.

### 3.3. Breakpoint determination and deletion mechanism

Although MLPA is effective to identify gross rearrangements within ATP7B, it could yield false positive results due to the possibility of polymorphisms on probe positions. In order to confirm MLPA results

and characterize intragenic deletions, the breakpoints of gross rearrangements were mapped using long-range PCR and sequencing analysis. We described the breakpoint locations in these patients, and the details were shown in Fig. 2B, C, D. Specifically, the breakpoints of exon 10-11 deletion were mapped to 1612-bp upstream of exon 10 and 31-bp downstream of exon 11, as well as an insertion of 12-bp in the junction breakpoint (c.2447 + 1612, 2730 + 31delins ATGGAAGGG AGG) (Fig. 2B). The 12-bp sequence matches with human genome (NCBI Build 38), and is found in all the chromosomes, except chromosome 13. Exon 2 deletion was also mapped (c.52-9329\_1286-11del) by primer walk (Fig. 2C). Two similar monoexonic deletions had been reported in two Chinese WD patients [12], but failing to determine the breakpoints.

For exons 18-21 deletion, sequencing analysis showed that the deletion covered 3925-bp region starting from 592-bp upstream of intron

**Table 1**  
Fifteen novel *ATP7B* variants identified in present study.

Site	Nucleotide mutation	Protein alteration	Sift		PolyPhen 2		1000g	ExAc	gnomAD	ACMG Classification	Evidence of Pathogenicity
			Score	Prediction	Score	Prediction					
intron1	c.51+2T > G	n.a.	n.a.	n.a.	n.a.	n.a.	0	0	0	P	PVS1 + PM2 + PM3 + PP4
exon2	c.171_174dup	p.T59Gfs*20	n.a.	n.a.	n.a.	n.a.	0	0	0	P	PVS1 + PM2 + PM3 + PP4
exon2	c.192_193dup	p.L65Sfs*4	n.a.	n.a.	n.a.	n.a.	0	0	0	P	PVS1 + PM2 + PM3 + PP4
exon2	c.326dup	p.Q110Afs*53	n.a.	n.a.	n.a.	n.a.	0	0	0	P	PVS1 + PM2 + PM3 + PP4
exon8	c.2212_2213 delinsCA	p.S738H	0	Damaging	0.838	Probably Damaging	0	0	0	LP	PM2 + PM3 + PP3 + PP4
exon10	c.2561A > T	p.E854V	0	Damaging	0.997	Probably Damaging	0	0	0	LP	PM2 + PM3 + PM5 + PP3 + PP4
exon11	c.2665C > G	p.H889D	0.001	Damaging	0.994	Probably Damaging	0	0	0	LP	PM2 + PM3 + PM5 + PP3 + PP4
exon11	c.2692C > T	p.Q898*	n.a.	n.a.	n.a.	n.a.	0	0	0	P	PVS1 + PM2 + PM3 + PP4
exon12	c.2817G > C	p.W939C	0	Damaging	1	Probably Damaging	0	0	0	P	PS1 + PM2 + PM3 + PP3 + PP4
exon13	c.3043C > A	p.L1015M	0	Damaging	0.999	Probably Damaging	0	0	0	LP	PM2 + PM3 + PM5 + PP3 + PP4
exon14	c.3181G > C	p.G1061R	0.001	Damaging	1	Probably Damaging	0	0	0	LP	PM2 + PM3 + PM5 + PP3 + PP4
exon17	c.3605C > A	p.A1202D	0	Damaging	0.997	Probably Damaging	0	0	0	LP	PM2 + PM3 + PM5 + PP3 + PP4
exon19	c.3932T > A	p.I1311N	0	Damaging	0.996	Probably Damaging	0	0	0	LP	PM2 + PM3 + PM5 + PP3 + PP4
intron20	c.4124+2T > G	n.a.	n.a.	n.a.	n.a.	n.a.	0	0	0	P	PVS1 + PM2 + PM3 + PP4
intron20	c.4124+4A > G	n.a.	n.a.	n.a.	n.a.	n.a.	0	0	0	VUS	PM2 + PM3 + PP4

**Abbreviations:** n.a. = not available; gnomAD = genome aggregation database; P = pathogenic; LP = likely pathogenic; VUS = variants with uncertain significance.

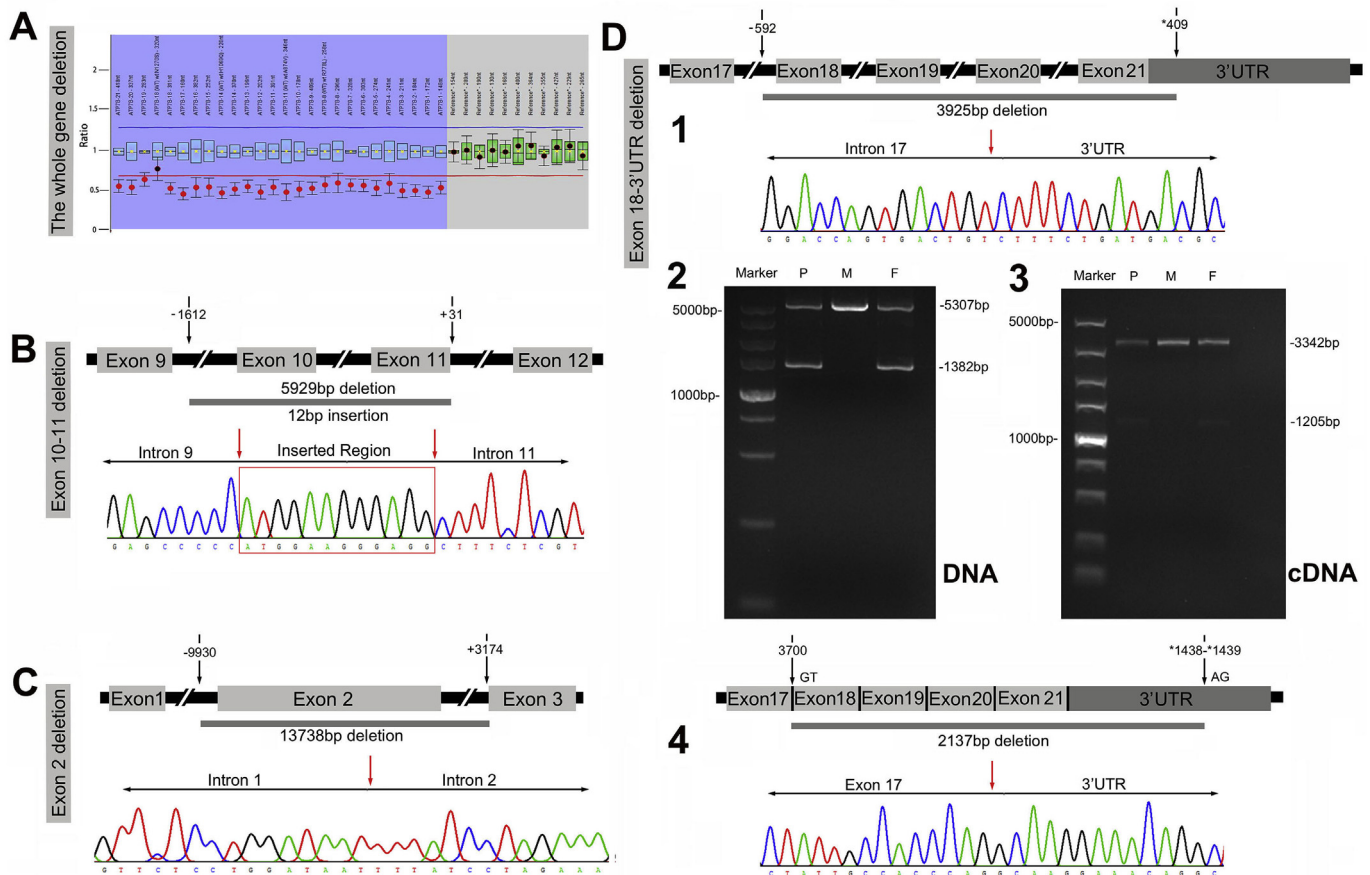


**Fig. 2. The breakpoint analysis of the four copy number variants.** **A.** MLPA assay for 5'UTR to exon 21 deletion. **B.** Schematic diagram of the exons 10-11 deletion (c.2447 + 1612\_2730 + 31delinsATGGAAGGGAGG) on DNA level. **C.** Schematic representation of the exon 2 deletion (c.52-9329\_1286-11del) on DNA level. **D1.** Schematic representation of the exons 18-3'UTR deletion (c.3700-592\_\*409del) on DNA level. **D2.** 2% agarose gel electrophoresis of the amplified products from the patient 5 (P), her mother (M), and her father (F) on DNA level. A 5307bp band is the normal fragment, and a 1382bp band is the aberrant product. **D3.** 0.8% agarose gel electrophoresis of the Long-Range PCR products from cDNA of index patient (P), her mother (M) or her father (F), respectively. A 3342bp band is the normal fragment, and a 1205bp band is the aberrant product. The maker is DL 5000 DNA Marker. **D4.** Schematic representation of the exons 18-3'UTR deletion (r.3700\_\*1439del) on cDNA level.

17 to 409-bp downstream of 3'UTR (Figs. 2D-1). This deletion was termed as c.3700-592\_\*409del at DNA level (Fig. 2D-2). To determine the impact of 3925-bp deletion on mRNA production, we performed reverse-transcription PCR (RT-PCR) analysis in the index patient as well

as her parents. Agarose gel electrophoresis showed an abnormal 1205-bp band in the proband and a normal 3342-bp band in the control (Figs. 2D-3). The findings revealed that the breakpoints could lead to dominantly acting splice-gain event, activating a cryptic AG donor

splice site in the nucleotide positions 1438-1439 of 3'UTR (Figs. 2D-4).

For exon 2 deletion, we observed only a 2-bp microhomology (AT) at the breakpoints (Supplemental Fig. 4A). Moreover, we analyzed the *ATP7B* sequence, and identified deletion regions which were flanked by an AluSc repeat at upstream of the 5' breakpoint and an AluJr repeat at downstream of the 3' breakpoint. After BLAST alignment, AluSc shared 73% homology with AluJr element. However, all sequences of AluSc and AluJr elements were completely detected around the breakpoint, hence excluding the possibility of homologous recombination. For exon 18-21 deletion, we also observed a 2-bp microhomology (GT) at the fusion breakpoint sequences (Supplemental Fig. 4B). In addition, we detected a 2-bp microhomology (CT) at fusion location of exon 10-11 deletion, and a 12-bp sequence insertion at the corresponding breakpoint area (Supplemental Fig. 4C).

#### 4. Discussion

The direct sequencing analysis enabled us to identify 71 variants among 142 WD patients, of which 15 variants were novel. These unreported variants considerably expanded the spectrum of *ATP7B* mutations. The pathogenic classifications of these novel variants could help to make the definitive genetic diagnosis. Some studies using the direct sequencing analysis demonstrated that the rate of genetic diagnosis of *ATP7B* did not reach to 100% among clinically diagnosed WD patients [4,13,15]. This genetic doubt could be due to the presence of intragenic rearrangements, which the direct sequencing could not identify.

MLPA technique was performed in this study to screen the gross rearrangements in *ATP7B*. Our result revealed 4 additional intragenic deletions. Combined with 10 previously reported mutations, a total of 14 intragenic rearrangements were found [5–12]. Among 10 reported intragenic mutations, only 6 various exons or combinations deletions had been mapped to breakpoint locations [5,6,8,11] (Table 2). None of these was detected in our cohort. In summary, our study expanded the spectrum of intragenic deletions within *ATP7B*. The MLPA technique indeed enhanced the rate of genetic diagnosis, despite the Results did not yet reach 100%. Among 142 current and 632 previous patients, 219 patients could receive a genetically definitive diagnosis, and 73 patients with one or none variant were still unclear. Despite the remaining 482 patients with compound heterozygous mutations did not undergo cosegregation analysis, they could be clinically diagnosed as WD according to the Leipzig Score. The reason may be due to some extragenic mutations, which were unable to be found by Sanger sequencing or

MLPA. For example, the deletion in the long arm of Chromosome 13 was observed in a 13-year-old boy, and this mutation involved the *ATP7B* gene, causing the WD phenotype [16].

Interestingly, we found a whole gene deletion in the patient who was previously considered as T935M homozygotes. Because of unknown deletion locations and the lack of family members, we failed to characterize these breakpoints at DNA level. The findings revealed that patients with homozygous mutations should be considered as potentially hemizygous state without parental genetic information.

Moreover, we also detected that intronic deletions could cause the generation of novel splice sites, and then affect *ATP7B* protein function. Two intronic deletions flanking normal copy number region were observed suggesting a potential genetic rearrangement [17]. Utilizing mRNA sequence analysis revealed that deep intronic deletions in both sides of affected exon could induce exon skipping, intron retention or insertion of sequence from others gene in mRNA transcript [18]. Combined with our Results, these findings emphasized that intronic deletions could be a kind of disease-causing mutation, although often masking their abnormalities at DNA level.

Gross deletions are often linked to repetitive elements spreading throughout the genome. Of the reported action elements, Alu-mediated gene rearrangements is the most common one [11]. Recent study has shown that Alu-element might be responsible for gross deletion in WD patients [10]. In order to investigate possible mechanism of intragenic deletions in the present study, DNA sequence flanking the breakpoints were analyzed. Moreover, it is well known that gross deletions often occur during DNA double strand breaks, which could be restored by non-homologous end joining (NHEJ). The NHEJ editing process involve either short microhomologies with often 1-4bp region, or sequence insertions. Because of the presence of Alu elements in the vicinity of the breakpoints, it could exclude Alu-mediated nonallelic homologous recombination. These findings supported that NHEJ could be the responsible mechanism for exon 2 deletion microhomology (AT). Similarly, the microhomology sequence (GT) were confirmed in the breakpoint region of exon 18-21 deletion. And patients with exon 10-11 deletion also showed both the presence of 2-bp microhomology (CT) and insertion of 12-bp sequences. Therefore, the NHEJ mechanism might explain the reasons for three different gross deletions.

#### 5. Conclusion

The current study considerably expanded the mutation spectrum of *ATP7B* and provided 15 novel genetic variants including 14 pathogenic

**Table 2**  
Unique *ATP7B* copy number variants identified to date.

Exons	Het/	Del/	Size (bp)	cDNA-based nomenclature	MicroHomology (bp)	Likely mechanism	Index	References
	Hom	Dup						
2	Het	Del	n.d.	c.52-?_1285 + ?	n.a.	n.a.	2	Rui Hua et al. [2016]
2	Het	Del	13738	c.52-9329_1286-11del	2	NHEJ	2	<b>Present study</b>
2	Hom	Del	3039	c.52-2671_368del	0	Alu-RT	1	Mameli et al. [2015]
2-4	Hom	Del	8798	c.51 + 384_1708-953del	4	NHEJ	1	Incollu et al. [2011]
4	Het	Del	n.d.	c.1544-?_1707 + ?	n.a.	n.a.	2	Muriel Bost et al. [2012]
5-6	Het	Del	n.d.	c.1708-?_1946 + ?	n.a.	n.a.	1	Møller et al. [2011]
6-8	Het	Del	3837	c.1870-45_2355 + 189del	3	NHEJ	1	Yasuaki Tatsumi et al. [2011]
10-11	Het	Del	5929	c.2447 + 1612_2730 + 31delins ATGGAAGGGAGG	2(12bp insertion)	NHEJ	2	<b>Present study</b>
14-16	Het	Del	4175	c.3134_3556 + 689del	6	MMEJ	1	Theodor Todorov et al. [2016]
17-19	Het	Del	3505	c.3556 + 281_4001del	4	NHEJ	1	Theodor Todorov et al. [2016]
20-21	Hom	Del	n.d.	c.4022-?_4398 + ?	n.a.	n.a.	1	Møller et al. [2011]
20	Hom	Del	2159	c.4021 + 87_4125-2del	2	NHEJ	1	Moller LB et al. [2005]
	Het, Hom						3, 2	Theodor Todorov et al. [2016]
18-3'UTR	Het	Del	3925	c.3700-592_*409del	2	NHEJ	1	<b>Present study</b>
5'UTR-21	Het	Del	n.d.	c.-157-?_*2087 + ?	n.a.	n.a.	1	<b>Present study</b>

**Abbreviations:** Het = Heterozygous; Hom = Homozygous; Del = deletion; Dup = Duplication; n.d. = not determined; n.a. = not available; Alu-RT = Alu retrotransposition; NHEJ = nonHomologous end joining; MMEJ = microhomologous end joining.

variants. Beyond the routine sequencing method, MLPA allowed us to detect four complex *ATP7B* intragenic deletions, and hence should be implemented in genetic testing for WD to avoid genetic diagnostic doubt. Moreover, the finding demonstrated that intragenic deletions of Chinese WD patients might not be an exceptionally rare event as well. By long-range PCR and sequencing analysis, we characterized three intragenic deletions, and found NHEJ as possibly causative mechanism causing intragenic deletions. Additionally, intronic deletion could be responsible for WD, and increased the complexity of *ATP7B* mutation.

#### Authors' roles

YCC, HY and RMW generated PCR, Sanger sequencing Results. YCC generated MLPA analysis and breakpoint mapping results. YCC, HY, RMW, YD and ZYW analyzed the data and advised on data analysis. JJX, WN and YZ helped to collect patients. YCC and HY drafted the manuscript, YD and ZYW reviewed and edited the manuscript. YD and ZYW designed the study and ZYW supervised all aspects of the study. All authors read and approved the final manuscript.

#### Funding

This work was supported by the grants, 81125009 (ZYW) and 81701126 (YD), from the National Natural Science Foundation (Beijing), and the research foundation for distinguished scholar of Zhejiang University to ZYW (188020-193810101/089, Hangzhou).

#### Financial disclosures/conflict of interest

The authors report no potential conflicts of interest.

#### Acknowledgements

We would like to thank all of the participants for their supports and willingness to participate in this study.

#### Appendix A. Supplementary data

Supplementary data to this article can be found online at <https://doi.org/10.1016/j.parkreldis.2019.01.001>.

#### References

[1] A. Ala, A. Walker, K. Ashkan, J. Dooley, M. Schilsky, Wilson's disease, *Lancet* 369

- (2007) 397–408.
- [2] R.E. Tanzi, K. Petrukhin, I. Chernov, J.L. Pellequer, W. Wasco, B. Ross, et al., The Wilson disease gene is a copper transporting ATPase with homology to the Menkes disease gene, *Nat. Genet.* 5 (1993) 344–350.
- [3] P. Ferenci, K. Caca, G. Loudianos, G. Mieli-Vergani, S. Tanner, I. Sternlieb, et al., Diagnosis and phenotypic classification of Wilson disease, *Liver Int. : Offic. J. Int. Assoc. Study Liver* 23 (2003) 139–142.
- [4] A.J. Coffey, M. Durkie, S. Hague, K. McLay, J. Emmerson, C. Lo, et al., A genetic study of Wilson's disease in the United Kingdom, *Brain* 136 (2013) 1476–1487.
- [5] L. Møller, P. Ott, C. Lund, N. Horn, Homozygosity for a gross partial gene deletion of the C-terminal end of *ATP7B* in a Wilson patient with hepatic and no neurological manifestations, *Am. J. Med. Genet.* 138 (2005) 340–343.
- [6] S. Incollu, M. Lepori, A. Zappu, V. Dessi, M. Noli, E. Mameli, et al., DNA and RNA studies for molecular characterization of a gross deletion detected in homozygosity in the NH2-terminal region of the *ATP7B* gene in a Wilson disease patient, *Mol. Cell. Probes* 25 (2011) 195–198.
- [7] L. Møller, N. Horn, T. Jeppesen, J. Vissing, F. Wibrand, P. Jennum, et al., Clinical presentation and mutations in Danish patients with Wilson disease, *Eur. J. Hum. Genet.* 19 (2011) 935–941.
- [8] Y. Tatsumi, T. Shinohara, M. Imoto, S. Wakusawa, M. Yano, K. Hayashi, et al., Potential of the international scoring system for the diagnosis of Wilson disease to differentiate Japanese patients who need anti-copper treatment, *Hepatol. Res.* 41 (2011) 887–896.
- [9] M. Bost, G. Piguat-Lacroix, F. Parant, C. Wilson, Molecular analysis of Wilson patients: direct sequencing and MLPA analysis in the *ATP7B* gene and *Atox1* and *COMMD1* gene analysis, *J. Trace Elem. Med. Biol.: Organ Soc. Miner. Trace Elem.* 26 (2012) 97–101.
- [10] E. Mameli, M. Lepori, F. Chiappe, G. Ranucci, F. Di Dato, R. Iorio, et al., Wilson's disease caused by alternative splicing and Alu exonization due to a homozygous 3039-bp deletion spanning from intron 1 to exon 2 of the *ATP7B* gene, *Gene* 569 (2015) 276–279.
- [11] T. Todorov, P. Balakrishnan, A. Savov, P. Socha, H. Schmidt, Intragenic Deletions in *ATP7B* as an Unusual Molecular Genetics Mechanism of Wilson's Disease Pathogenesis, *PLoS One* 11 (2016) e0168372.
- [12] R. Hua, F. Hua, Y. Jiao, Y. Pan, X. Yang, S. Peng, et al., Mutational analysis of *ATP7B* in Chinese Wilson disease patients, *Am. J. Transl. Res.* 8 (2016) 2851–2861.
- [13] Y. Dong, W. Ni, W. Chen, B. Wan, G. Zhao, Z. Shi, et al., Spectrum and classification of *ATP7B* variants in a large cohort of Chinese patients with Wilson's disease guides genetic diagnosis, *Theranostics* 6 (2016) 638–649.
- [14] S. Richards, N. Aziz, S. Bale, D. Bick, S. Das, J. Gastier-Foster, et al., Standards and guidelines for the interpretation of sequence variants: a joint consensus recommendation of the American College of medical genetics and Genomics and the association for molecular pathology, *Genet. Med.* 17 (2015) 405–424.
- [15] I.J. Chang, S.H. Hahn, The genetics of Wilson disease, *Handb. Clin. Neurol.* 142 (2017) 19–34.
- [16] D. Riley, M. Wiznitzer, S. Schwartz, A. Zinn, A 13-year-old boy with cognitive impairment, retinoblastoma, and Wilson disease, *Neurology* 57 (2001) 141–143.
- [17] B. Baskin, D. Stavropoulos, P. Rebeiro, J. Orr, M. Li, L. Steele, et al., Complex genomic rearrangements in the dystrophin gene due to replication-based mechanisms, *Mol. Genet. Genomic Med.* 2 (2014) 539–547.
- [18] B. Baskin, W. Gibson, P. Ray, Duchenne muscular dystrophy caused by a complex rearrangement between intron 43 of the *DMD* gene and chromosome 4, *Neuromuscul. Disord.* 21 (2011) 178–182.